Assessment of ordered and complementary pore volumes in polymer-templated mesoporous silicas and organosilicas†

Mietek Jaroniec*[a] and Leonid A. Solovyov[b]

Received (in Cambridge, UK) 23rd March 2006, Accepted 18th April 2006
First published as an Advance Article on the web 3rd May 2006
DOI: 10.1039/b604283j

A method to determine the volumes of ordered mesopores and complementary small pores in polymer-templated ordered mesoporous silicas and organosilicas is proposed on the basis of the existing relation between the pore width and unit cell values obtained by the XRD structure modeling and the adsorption pore volume.

A major breakthrough in the area of ordered mesoporous materials (OMMs) that emerged after the discovery of surfactant-templated silicas such as MCM-41 and MCM-48,[1] was the synthesis of block copolymer-templated silicas such as SBA-15 and SBA-16.[2] These ordered mesoporous silicas (OMSs) have received a great deal of attention because they usually exhibit larger mesopores, thicker pore walls and higher hydrothermal stability than their surfactant-templated counterparts. A variety of polymer-templated ordered mesoporous silicas (PTOMSs) have been synthesized including channel-like mesostructures such as SBA-15[2] (*P6m*) and KIT-6[3] (*Ia3d*) as well as cage-like mesostructures such as SBA-16[2] (*Im3m*) and FDU-1[4] (*Fm3m*). A characteristic feature of OMSs prepared in the presence of block copolymers containing poly(ethylene oxide) segments, which differentiates them from surfactant-templated OMSs, is the presence of complementary irregular micropores in the walls of ordered mesopores.[5] These micropores provide interconnections between 2-D hexagonally ordered cylindrical mesopores of SBA-15 and in fact this material has a 3-D mesoporous–microporous structure.[5] In cage-like PTOMSs, in addition to the complementary micropores present in the mesopore walls, each cage is connected with neighboring cages *via* eight (*Im3m*) or twelve (*Fm3m*) ordered apertures.[2,4] Experimental studies of PTOMSs show that the estimation of the volume of ordered mesopores as well as the volume of complementary micropores and ordered interconnections (in the case of cage-like OMSs) is a difficult task.[6] For instance, stable inverse carbon replicas of SBA-15 were obtained, although *t*-plot or α_s-plot analysis showed a very small volume of complementary micropores.[7] Similarly, analysis of porosity by using the existing methods to evaluate the pore size distribution (PSD) for cage-like PTOMSs is complex because mesocages are spherical and interconnecting pores are rather channel-like.

[a]*Department of Chemistry, Kent State University, Kent, Ohio, 44242, USA. E-mail: jaroniec@kent.edu; Fax: 1 330 672 3816; Tel: 1 330 672 3790*
[b]*Institute of Chemistry and Chemical Technology, 660049, Krasnoyarsk, Russia*

† Electronic supplementary information (ESI) available: Three figures and one table with SAXS data and parameters, respectively; two figures with nitrogen adsorption isotherms and pore size distributions for SBA-15. See DOI: 10.1039/b604283j

Therefore, there is a need for an independent and accurate assessment of the volume of ordered mesopores as well as the volume of complementary pores in PTOMSs. Since for each ordered mesostructure there is a unique relation between the pore width, unit cell parameter and volume of ordered mesopores, here we propose to estimate the latter volume from this relation by using the unit cell and pore-width values determined by the X-ray diffraction (XRD) structure modeling. It has been shown recently[8] that the XRD structure modeling is a powerful tool allowing an accurate reproduction of experimental XRD patterns for various mesostructures and, consequently, permitting an accurate determination and analysis of their structural parameters.

Analytical expressions defining the relation between the pore width, unit cell parameter and volume of ordered mesopores have been derived for *P6m*,[9] *Ia3d*,[10] *Im3m*,[11] *Fm3m*[12] and related mesostructures. For instance, for 2-D hexagonally ordered mesopores (*P6m* symmetry) this relation is as follows:[9]

$$w = c_h\, a[V_o/(1/\rho + V_o)]^{1/2} \quad (1)$$

where w is the pore width, a is the unit cell parameter, V_o is the volume of ordered mesopores, ρ is the density of silica framework, and c_h is the characteristic constant for 2-D hexagonal mesostructure (*P6m*). This constant is equal to $[(2 \times 3^{1/2})/\pi]^{1/2} = 1.050$ for cylindrically shaped mesopores and 1.0 for the hexagonally shaped channels. Eqn (1) is valid for OMSs such as MCM-41, which do not possess additional (complementary) pores in the mesopore walls. For OMSs such as SBA-15, which contain complementary pores in the mesopore walls, the denominator of eqn (1) should contain V_{co} instead of V_o, where V_{co} is the sum of the volumes of complementary pores, V_c, and ordered mesopores, V_o:

$$V_{co} = V_c + V_o \quad (2)$$

Thus, an analogue of eqn (1) for polymer-templated *P6m* mesostructures such as SBA-15 is:[13]

$$w = c_h\, a[V_o/(1/\rho + V_{co})]^{1/2} \quad (3)$$

Analogous equation to eqn (3) has been derived for cage-like PTOMSs such as SBA-16 (*Im3m*)[11] and FDU-1 (*Fm3m*):[12]

$$w = c_c\, a[V_o/(1/\rho + V_{co})]^{1/3} \quad (4)$$

where c_c is the characteristic constant for cage-like cubic mesostructures; it is equal to 0.985 for body-centred-cubic

(*Im*3*m*) symmetry[11] and 0.782 for face-centred-cubic (*Fm*3*m*) symmetry.[12]

The pore volume V_{co}, which includes the volume of ordered mesopores as well as the volume of complementary pores (*i.e.*, micropores present in the mesopore walls and in the case of cage-like materials, interconnecting ordered apertures between neighbouring ordered cages), can be relatively easily estimated from adsorption isotherm measured for nitrogen, argon or other related adsorbate. Note that the pore volume V_{co} includes ordered mesopores and all complementary pores present in the mesopore walls and smaller than ordered mesopores. This value can be estimated directly from adsorption isotherm by converting the amount adsorbed at the isotherm plateau, which appears after steep step reflecting capillary condensation in ordered mesopores, to the volume of liquid adsorbate (see Fig. S4 in the ESI).† Alternatively, this volume can be estimated: (i) by α_s-plot or *t*-plot analysis by converting the intercept of the linear segment of this plot, which appears after aforementioned condensation step, to the volume of liquid adsorbate,[14] or (ii) by integration of the differential PSD evaluated by the DFT,[15] KJS[16] or other related methods over the pore range including complementary small pores and ordered mesopores. Since the PSD curves for OMSs exhibit a distinct peak for ordered mesopores, the identification of the upper limit of integration is an easy task. If an accurate PSD is available in the entire pore range, the amount of complementary pores can be estimated by integration of PSD at the proper range; however, the evaluation of PSD in the micropore range is still a very difficult task. Therefore, an independent assessment of complementary porosity in OMSs is an important issue for quantitative characterization of these exciting nanostructures.

Having the value V_{co} (estimated from adsorption data) and estimating the unit cell parameter *a* and pore width *w* by the XRD structure modeling[8], one is able to evaluate the volume of ordered mesopores for various mesostructures by using equations, which are another forms of eqns (3) and (4):

$$V_o = [w/(c_h\, a)]^2\, (1/\rho + V_{co}) \quad (5)$$

$$V_o = [w/(c_c\, a)]^3\, (1/\rho + V_{co}) \quad (6)$$

and eqn (5) is applicable for *P6m* mesostructures, whereas eqn (6) is for *Im*3*m* and *Fm*3*m* cubic mesostructures.

To illustrate the validity of these relations, eqn (1) was examined for a series of MCM-41 samples reported previously.[17] The XRD patterns reported for these samples in a previous work[17] were modelled to evaluate the unit cell parameter and pore width by assuming the hexagonal shape of mesopores and using the Debye–Waller factor of 4 nm^2, which is characteristic for MCM-41-type OMS.[8] The XRD full-profile refinement was performed by using the derivative difference minimization (DDM) method.[18] The resulting values from the XRD analysis are summarized in Table 1 in comparison with the pore width values reported in the previous work,[17] which were estimated by eqn (1) (*i.e.*, using the unit cell parameter obtained from the (100) XRD reflection for the *P6m* symmetry group and the volume of ordered mesopores from the α_s-plot analysis). Note that the latter values can be up to 5% larger because they were calculated for cylindrically-shaped mesopores (c_h = 1.05).[17] An illustration of the XRD profile fitting is shown in ESI Fig. S1 for the MCM-41-C18 sample. A comparison of the data in Table 1 shows a very good agreement of the pore width values obtained by the XRD analysis and eqn (1); note that the former values are obtained from the XRD data only, whereas the latter values are calculated from eqn (1), which requires the unit cell parameter (or the XRD d_{100} spacing) and the volume of ordered mesopores estimated from nitrogen adsorption isotherm. The density of silica framework was assumed to be 2.2 g cm^{-3}.[17] This nice agreement between the XRD structure modelling and the data obtained by eqn (1) was expected because the MCM-41 samples studied did not have microporosity.

Table 1 Structural parameters of the MCM-41 samples

	XRD modelling			
MCM-41[a]	*a*/nm	*w*/nm	*w* (eqn (1))/nm	w_{KJS}/nm
C12	4.04	3.07	3.10	3.07
C14	4.43	3.53	3.53	3.46
C16	4.81	3.99	3.93	3.80
C18	5.27	4.44	4.20	4.20
C20	5.44	4.47	4.40	4.42
C22	5.95	5.00	4.88	4.86

[a] Details about synthesis of the MCM-41 samples can be found elsewhere;[17] MCM-41-C16 refers to the C16-7 sample. The two last columns provide data reported previously.[17]

To illustrate the proposed method for evaluation of the volumes of ordered and complementary pores in PTOMSs we used some of the recently reported data for the SBA-15[19] and SBA-16[20] silicas as well as for the SBA-15[21] and SBA-16[22] organosilicas containing ethane and isocyanurate bridging groups, respectively. For the SBA-15 samples we used eqn (5), whereas the SBA-16 samples were analyzed by applying eqn (6). For all of these samples the small angle X-ray scattering (SAXS) data reported in the aforementioned papers were used.[19–22] The density distribution in SBA-16 was modeled by the body centred cubic arrangement of spherical areas of zero density with a constant density between the areas.[20,23] The DDM refinement allowed us to evaluate the unit

Table 2 Adsorption and structural parameters for the PTOMSs samples studied

	SAXS modelling				
PTOMS[a]	*a*/nm	*w*/nm	V_{co}/cc g^{-1}	V_o/cc g^{-1}	V_c/cc g^{-1}
SBA-15/06	11.66	8.63	1.03	0.73	0.30
SBA-15/24	12.12	9.39	1.11	0.85	0.26
SBA-15/72	12.43	10.02	1.12	0.92	0.20
SBA-15/96	12.45	10.10	1.16	0.96	0.20
SBA-15/12*	12.29	9.72	1.12	0.89	0.23
SBA-15/48*	11.98	9.87	1.12	0.94	0.18
SBA-15/72*	12.44	10.37	1.11	0.98	0.13
SBA-15-E	12.97	9.00	1.09	0.76	0.33
SBA-16	13.80	7.40	0.47	0.15	0.32
SBA-16-ICS	17.11	9.40	0.56	0.21	0.35

[a] Data for the SBA-15 (samples without * were hydrothermally treated at 100 °C, those with * were treated at 120 °C) and SBA-16 silicas were taken from ref. 19 and 20; data for the SBA-15-E and SBA-16-ICS containing ethane and isocyanurate bridging groups, respectively, were taken from ref. 21 and 22; the volumes V_{co} for the SBA-15 samples were evaluated by α_s-plot analysis (note the volumes V_{co} reported in ref. 19 are slightly different because they were evaluated by integration of the KJS PSD curve) and for the SBA-16 samples from the isotherm plateau. The cylindrical shape of pores was assumed for SBA-15 samples. The density of 2.2 g cm^{-3} was used for silica samples, and 1.5 g cm^{-3} for ethane–silica[21] and isocyanurate–silica.[22]

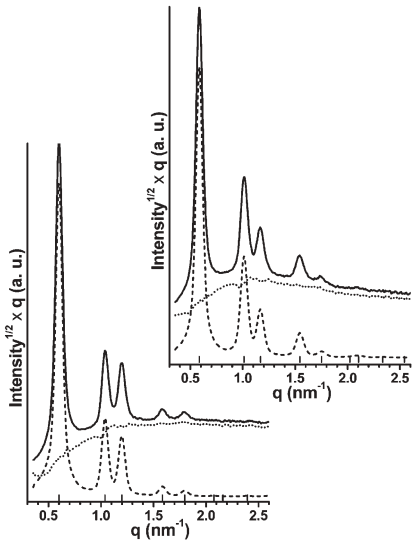

Fig. 1 The weighted and Lorentz-corrected observed (solid line), calculated (dashed line), and difference (dotted line) SAXS patterns for samples SBA-15/24 (left) and SBA-15-72* (right) after DDM full-profile structure refinement; the calculated diffraction reflection positions are marked by inward ticks.

cell parameters and the widths of ordered mesopores (see data in Table 2 and ESI Table S1).† Fig. 1 and ESI Fig. S2 and S3† show the SAXS full-profile fitting for one SBA-15 silica and two organosilica samples; the SAXS data for these samples are reported elsewhere.[19,21,22] For illustration, Fig. 2 shows the density distribution image for the SBA-16 organosilica with isocyanurate bridging groups.

Table 2 contains, in addition to the unit cell and pore width values obtained by the SAXS modelling, the values of the pore volume values, V_{co}, which were obtained from nitrogen adsorption isotherms by the α_s-plot analysis, as well as the volumes of ordered mesopores determined by eqn (5) for SBA-15 mesostructures and eqn (6) for SBA-16 mesostructures. This table contains also the volumes of complementary pores evaluated on the basis of eqn (2). A comparison of the volumes of complementary pores reported in this work with those evaluated by the integration of the KJS PSD curves for the SBA-15 samples up to 3 nm [19] shows that the values given in Table 2 are larger, which is logical because the KJS method has a limited applicability for the analysis of microporosity (it was calibrated for the mesopore range from 2 to 6.5 nm [16]). In addition, the proposed method gives the volume of pores smaller than the ordered mesopores, while the pore volumes reported previously[19] were obtained by integration of the KJS PSD curve up to 3 nm only. If this integration is done over a larger range of pore widths (for instance, see the KJS PSD curve for SBA-15/06 in ESI Fig. S5),† the volume $V_c = 0.34$ cc g^{-1} is obtained instead of 0.20 cc g^{-1} (integration up to 3 nm), which is much closer to the value of 0.30 cc g^{-1} determined by eqn (5).

In conclusion, this work shows that the currently available methods of XRD structure modelling are especially suitable for an accurate evaluation of the lattice parameters and the pore widths of polymer-templated OMSs. The use of these values in expressions such as eqns (4) and (5) that define the relation between the pore width, unit cell, and pore volume for a given type

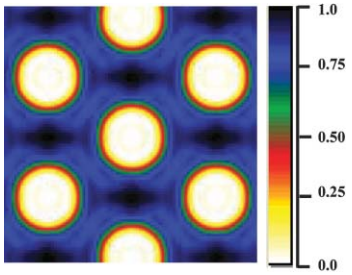

Fig. 2 The (110) section of density distribution for the SBA-16 silica containing isocyanurate based on the intensities determined from the observed SAXS pattern by the DDM decomposition.

of mesostructure allows one to determine the volumes of ordered mesopores and complementary pores. This method is particularly useful for polymer-templated cage-like silicas and organosilicas because for those materials the analysis of the intrawall microporosity as well as the mesopore interconnecting apertures is especially difficult.

The support of NSF Grant CHE-0093707 (M.J.) and RFBR Grant 03-03-32127 (L.A.S.) is acknowledged.

Notes and references

1 C. T. Kresge, M. E. Leonowicz, W. J. Roth, J. C. Vartuli and J. S. Beck, *Nature*, 1992, **359**, 710.
2 D. Zhao, J. Feng, Q. Huo, N. Melosh, G. H. Fredrickson, B. F. Chmelka and G. D. Stucky, *Science*, 1998, **279**, 548.
3 F. Kleitz, S. H. Choi and R. Ryoo, *Chem. Commun.*, 2003, 2136.
4 C. Yu, Y. Yu and D. Zhao, *Chem. Commun.*, 2000, 575.
5 R. Ryoo, C. H. Ko, M. Kruk, V. Antochshuk and M. Jaroniec, *J. Phys. Chem. B*, 2000, **104**, 11465.
6 S. H. Joo, R. Ryoo, M. Kruk and M. Jaroniec, *J. Phys. Chem. B*, 2002, **106**, 4640.
7 H. J. Shin, R. Ryoo, M. Kruk and M. Jaroniec, *Chem. Commun.*, 2001, 349.
8 L. A. Solovyov, S. D. Kirik, A. N. Shmakov and V. N. Romannikov, *Microporous Mesoporous Mater.*, 2001, **44**, 17; L. A. Solovyov, O. V. Belousov, R. E. Dinnebier, A. N. Shmakov and S. D. Kirik, *J. Phys. Chem. B*, 2005, **109**, 3233.
9 M. Kruk, M. Jaroniec and A. Sayari, *J. Phys. Chem. B*, 1997, **101**, 583.
10 P. I. Ravikovitch and A. Neimark, *Langmuir*, 2000, **16**, 2419.
11 J. R. Matos, L. P. Mercuri, M. Kruk and M. Jaroniec, *Langmuir*, 2002, **18**, 844.
12 J. R. Matos, M. Kruk, L. P. Mercuri, M. Jaroniec, L. Zhao, T. Kamiyama, O. Terasaki, T. J. Pinnavaia and Y. Liu, *J. Am. Chem. Soc.*, 2003, **125**, 821.
13 M. Kruk, M. Jaroniec and A. Sayari, *Chem. Mater.*, 1999, **11**, 492.
14 A. Sayari, P. Liu, M. Kruk and M. Jaroniec, *Chem. Mater.*, 1997, **9**, 2499.
15 P. I. Ravikovitch, G. A. Haller and A. Neimark, *Adv. Colloid Interface Sci.*, 1998, **76**, 203.
16 M. Kruk, M. Jaroniec and A. Sayari, *Langmuir*, 1997, **13**, 6267.
17 M. Jaroniec, M. Kruk, H. J. Shin, R. Ryoo, Y. Sakamoto and O. Terasaki, *Microporous Mesoporous Mater.*, 2001, **48**, 127.
18 L. A. Solovyov, *J. Appl. Crystallogr.*, 2004, **37**, 743; L. A. Solovyov, A. M. Astachov, M. S. Molokeev and A. D. Vasiliev, *Acta Crystallogr., Sect. B*, 2005, **61**, 435.
19 P. F. Fulvio, S. Pikus and M. Jaroniec, *J. Mater. Chem.*, 2005, **15**, 5049.
20 T. W. Kim, R. Ryoo, K. P. Gierszal, M. Jaroniec, L. A. Solovyov, Y. Sakamoto and O. Terasaki, *J. Mater. Chem.*, 2005, **15**, 1560.
21 R. M. Grudzien, S. Pikus and M. Jaroniec, *J. Phys. Chem. B*, 2006, **110**, 2972.
22 R. M. Grudzien, B. E. Grabicka, S. Pikus and M. Jaroniec, *Chem. Mater.*, 2006, **18**, 1722.
23 F. Kleitz, L. A. Solovyov, G. M. Anilkumar, S. H. Choi and R. Ryoo, *Chem. Commun.*, 2004, 1536.

